EFFECT OF THERMAL LOADING ON CONTAINMENT CAPACITY

Dr N K Prinja, BSc, MSc, PhD, FIMechE, and J. A. Curley, BSc

AMEC Nuclear Limited, Knutsford, UK

ABSTRACT

This paper presents the assessment of concrete containment capacity for phase 3 of the International Standard Problem, ISP 48. The mandatory load case for phase 3 (Case 1) involving saturated steam conditions was analysed by using a full 3D global model of the containment structure. Heat transfer and nonlinear stress analysis was conducted using version 6.4 of ABAQUS to study the influence of thermal loading on the containment capacity. In addition, the effects of Thermal Transient Creep (TTC) in concrete at elevated temperatures have been investigated. It is concluded that the thermal straining of the liner results in rupture at approximately 1.25MPa, which is 14% higher than the rupture pressure of 1.1MPa obtained from the limit state test. The structural collapse dictated by the failure of the pre-loaded tendons also increases by 7% from 1.4MPa to 1.5MPa. Inclusion of thermal loading and temperature dependent effect of TTC show that the margin between the liner rupture and the structural collapse decreases.

INTRODUCTION

NRC/NUPEC sponsored tests of the ¼ scale pre-stressed concrete containment vessel (PCCV) which have been executed at Sandia National Laboratories (SNL) in the USA [1]. The Limit State Test (LST) executed during September 2000 was based on pneumatic pressurisation of the vessel and achieved a maximum pressure of 1.3MPa (3.3 times the design pressure). The objectives of the ISP48 are to extend the understanding of capacities of actual containment structures based on the results of the PCCV LST and any other sources of available research.

NNC participated in the LST round robin exercise and completed the analysis [2] to predict the limit load of the vessel. Predictions from all the participants of the round robin were collated and published by SNL in August 2000[3]. The LST identified liner tearing as the mode of failure. Whilst there was no visible damage to the PCCV structure, the breach of the pressure boundary dictated the limit load due to excessive leakage rate. It can be seen from Ref 3 that out of the total 17 participants, the NNC/HSE model is one of only four that successfully predicted liner tearing as the mode of failure. It was recognised at the international pre-test round robin meeting in October 1999 that the NNC/HSE model was one of the most sophisticated 3D full global models, which took account of the interaction between all the main structural features.

Following the pre-test round robin, NNC carried out the post-test analysis under HSE contract CE/GNSR/1 and the work was presented in Ref 4. This work consisted of a comparison between the FE analysis and the test results to give an assessment of the accuracy and reliability in predicting the failure modes and limit loads of PCCV structures using finite element analysis. It also included analysis of the Structural Failure Mode Test (SFMT) executed in November 2001, in which hydraulic pressure was used to over pressurise the containment to total structural collapse. The results of the over pressurisation test have been published by SNL[3]. The analysis carried out in Ref 2 predicted the failure location and the behaviour up to collapse with good accuracy.

All the previous test and analysis work done has shown that leakage occurs before the burst pressure but in these studies only the mechanical loading (gravity, prestress and internal pressure) was considered and thermal loading was ignored. In real containments, increase in internal pressure is associated with thermal loading. One of the aims of Phase 3 of the ISP48 project is to study the effects of accident temperatures and see if the onset of leakage is closer to the burst pressure in full size containments.

The 2nd meeting of the ISP48 project held in Spain in March 2004, reviewed Phase 2 results and finalised the combination of mechanical and thermal loadings for Phase 3[5]. The mandatory Case 1 consists of applying saturated steam conditions as steady state static loading and recommended Case 2 simulates Station Blackout pressure and temperature transients. This work covers only Case 1 of Phase 3.

PCCV FINITE ELEMENT MODEL

Description of the Global Model

All the Concrete components of the vessel are represented with the eight-noded solid elements type C3D8 [6]. The eight-node solid element includes smeared steel reinforcements. The origin of the FE model is at the centre of the top surface of the basemat. Directions 1, 2 and 3 are X, Y and Z respectively. X is along the 90° azimuth, Y is vertical and Z is along the 180° azimuth.

The mesh density of the cylinder wall and dome in the circumferential direction was driven by the requirement to model each vertical post-tensioning tendons explicitly. The resulting layout consists of a cylinder and dome wall mesh with elements at approximately 2° intervals in the circumferential direction. Three elements were employed in the wall-

thickness direction of the cylinder and dome. The mesh density in the vertical direction was influenced by the specification of the hoop tendons in the concrete elements. The cylinder hoop tendons were arranged at vertical intervals of 112.7mm. The solid element nodes are meshed vertically to correspond with the spacing of the hoop tendons.

The cylinder wall penetrations and their immediate vicinity have been modelled in detail. Structural features within the penetration area that are represented explicitly in the model are the enhanced reinforcement stiffening, thickened wall section (airlock and equipment hatch penetrations), steel plates lining the penetration cavity, the penetrations cover plates, the deviation in the layout of the vertical and hoop tendons, internal vessel liner and the liner anchorage.

The Prestressing System

The post-tensioning tendons have been modelled using two different approaches. The vertical tendons were modelled explicitly using the two-node, linear truss element T3D2. The hoop tendons are modelled as single rebars embedded within concrete elements

The load distribution within the tendons was non-uniform because of friction between the tendons and ducts. This was taken into account during the analysis by using the design values of the anchorage loads of 350kN and 471kN for the hoop and vertical tendons respectively. Variation in the tendon loads due to frictional loss was obtained by applying the following Equation 1.

$$P = P_{1,2}\, e^{(-\mu\beta - 0.001L)} \tag{1}$$

Where

$P_{1,2}$ = Load at the tensioning end 1 or 2.
β = Change of angle from tensioning end.
P = Load at β from tensioning end.
μ = Friction Coefficient. (taken as 0.21)
L = Length of Tendon.

The average seating loss of 24757N was taken from the PCCV test results, and was included in the calculations for the pre-loads. The modelling assumed that the seating loss was linear throughout the 90° segment.

Internal Liner and Liner Anchorages

The thicker insert plates surrounding the main steam and feed water penetrations are simulated with the shell element S4R and the general area of the liner with membrane type M3D4R elements.

The spring stiffness values are derived from test results for the pullout of anchorage plates in tensile and shear modes [1].

Concrete Reinforcements

The grid of reinforcing bars in the vessel has been represented as rebar smeared within the parent solid elements. The orientation, cross-sectional area, spacing and material properties are taken from the construction drawings [7].

The duct-supporting steel frame construction is modelled as single rebars within the parent solid elements. The properties of the steel frame are given in Ref 5.

PCCV Support Conditions

The basemat is constructed on a 150mm thick un-reinforced slab which itself is supported on an engineered sand and gravel subgrade. The soil stiffness was characterised as exhibiting a settlement of less than 25mm due to a bearing pressure of 3.11kN/m^2 [7].

The soil was represented using grounded spring elements (SPRING1). Each node on the bottom surface of the basemat was supported on a spring element. The spring stiffness was computed based on the influence area of each spring node. The vessel was constrained to eliminate rigid body translations and rotations at four nodal positions on the top surface of the basemat in the horizontal degrees of freedom.

Loading Data

The temperature loading for Case 1 is a steady state non-linear increase from 100°C to 200°C. The temperature loading was defined over a period of approximately 42 minutes, which was a pseudo time step as this heat transfer analysis was performed at steady state increments of temperature.

The pressure loading was a linear increase from 0MPa to 1.46MPa over the 42 minute pseudo time step.

Heat Transfer Modelling

In order for the model to be used for heat transfer analysis some modifications were required. These are highlighted below.

All concrete solid elements were replaced with corresponding heat transfer DC3D8 and DC3D6 elements, these include both the full and reduced integration continuum elements. This is because there are no reduced integration heat transfer elements available for 8 noded continuum elements.

The liner elements (which were M3D4 & M3D3 membrane elements) were replaced by S4 and S3 shell elements respectively. Even though the shell elements provide an in plane stiffness this was satisfactory as the stiffness can be neglected for heat transfer analysis.

The vertical tendons were previously modelled using T3D2 truss elements, for heat transfer analysis the element type had to be modified to DC1D2 (1D solid) elements. These elements were then attached to the concrete using equations to couple the temperature degrees of freedom. The hoop tendons and rebars were previously smeared into the solid elements using the *REBAR facility within ABAQUS. This type of element cannot be used during heat transfer and as there was no direct solution to this problem the hoop tendons and rebars were omitted for the heat transfer analysis. However the nodal temperatures are applied to the rebars and tendons during the stress analysis.

Boundary Conditions

Boundary conditions applied are as follows:-

- Sink Temperature of 25°C outside the PCCV.
- Convection from the outer surfaces of the cylinder, dome and exposed sections of the basemat concrete to free air.
- Convection from the insulated bottom surface of the basemat to the soil.

Conduction between Liner and Inner Concrete

To facilitate Conduction between the liner and the concrete, surfaces were created on the outer surface of the liner and the inner surface of the concrete so that a gap conduction could be set up. Gap conductivity uses the two surfaces and a specified conductivity depending upon distance between the two surfaces. The conductivity was set as a perfect thermal contact. Therefore between the two surfaces the thermal conductivity was defined as being the same as the conductivity of steel irrespective of distance between the surfaces.

Convection from Outer Concrete Surfaces

Two separate regions were specified for the convection from the outer surface of the concrete. Firstly one region was defined for the dome, cylinder and exposed sections of the basemat (i.e. top and sides) to allow for standard convection. Secondly the base of the basemat was defined as a surface to simulate conduction from the basemat into the soil. The equations for the convection from the outer surfaces were provided by SNL and are shown below:-

Convection to free air $h = 4.80 * (\Delta T)^{1/3}$ W/m^{0}K (2)

Convection into soil $h = 0.0724$ W/m^{0}K (3)

Effects of radiation have been ignored.

Thermal Loading

The heat transfer analysis was completed in two steps. The first step was a steady state heat transfer step in which the liner temperature was raised from 20°C to 100°C.

The second step raised the liner temperature in accordance with the temperature profile distributed by SNL. Each increment of the second step was converged as a steady state using the 42.23 minute pseudo time step as defined in the original SNL heat transfer analysis. By performing the heat transfer analysis in this way the pressure loading can be run as a time history using steady state temperatures at each increment of pressure.

ANALYSIS PROCEDURE

The stress analysis model was loaded as follows:-

Step 1 – Application of prestressing

Step 2 – Increase model temperature from 20°C to 100°C steady state

Step 3 – Apply temperature and pressure loading as defined by SNL

Steps 2 & 3 of the stress analysis model read in the nodal temperatures from the heat transfer analysis and are applied at each increment as a steady state temperature.

RESULTS AND ASSESSMENT

For the ISP 48 project the number of standard output locations have been reduced to 23 locations. For each location, the following results were obtained from the following are plotted:

- LST test results (pressure only) from Ref 1.
- FE analysis pressure only.
- FE analysis pressure plus temperature.
- FE analysis pressure plus temperature with TTC.

For sake of brevity, results at standard output location 39 and 53 are presented in Figures 1 to 3. The results are plotted against pressure. The finite element model has the initial values reset to line up with the Limit State Test results.

Assessment of the Liner

The primary function of the steel liner is to act as the pressure boundary for the containment. Therefore it is important to know the pressure it can sustain before rupture. It is the design intent that liner rupture and pressure leakage occurs at levels below that required to cause catastrophic failure of the concrete containment. The limit state test [1] demonstrated this design feature. Liner rupture was the first failure mode and the high leak rates seen ensured the concrete containment did not fail catastrophically.

The limit state test [1] did not consider the effects of accident temperature transients. Under such conditions, liner thermal expansion could influence the limit load before rupture. If liner thermal expansion is constrained by the concrete containment, compressive strains may be induced in the liner that increases the pressure required to cause rupture. From a design viewpoint, the concern is that the pressure required for liner rupture may increase to levels above that which causes structural failure of the vessel.

Figure 1 (location 39) presents the mechanical strain (total strain – thermal strain) in liner in the hoop direction midway up the cylinder wall, at the 135° azimuth. This figure highlights decreased strains are calculated in the liner when the thermal loading is included. These are indicative of compressive stress developed in the liner (see Figure 2) due to the differential thermal expansion. Assuming the liner rupture strain the same as that observed during LST (0.0015), the data indicates that the rupture pressure is increases by 0.15MPa when thermal expansion is included (see Figure 1). The results indicate that as expected, the liner is under compression initially due to the differential thermal expansion but begins to experience tensile stress after the cracking of the concrete.

Tendon Assessment

Ultimate structural collapse of the PCCV test model was initiated by failure of hoop tendons located in the free field region, approximately mid-height to the cylinder wall. Tendon failures resulted in a loss of pre-load to the concrete in this region and a breach of the wall ensued. It is therefore important to assess if the application of accident temperatures reduces the pressure at which rupture of the tendons occurs. Two aspects are assessed.

The first aspect is the temperature of the tendons during the fault. A significant increase could lower the material yield strength. Figure 4 presents a profile of the temperature distribution through the cylinder wall of the vessel. This shows the peak fault temperature of 200°C is transferred through the liner to the inner surface of the wall. However, the temperature quickly reduces through the wall thickness due to the insulating properties of the concrete. The hoop tendons are located in the wall, approximately 216mm from the inner surface. At this location the temperature approximates to a range between 100°C to 130°C and therefore is well below the level required to reduce the material yield strength [9].

The second aspect of vessel response considered is its global response when accident temperatures are included. Thermal expansion of the vessel could increase the prestress in the tendons and increases the pressure required to cause rupture. Figure 3 presents the mechanical strain (total strain – thermal strain) histories for the hoop tendon located at an elevation of 4.57m, mid-way between the equipment and airlock hatches. This is the region of vessel rupture from the structural failure test. The figure highlights that at the vessel rupture pressure of 1.4MPa, a tendon strain of 0.0034 is induced when only pressure is applied. For the pressure plus temperature case, a tendon strain of 0.0034 equates to a pressure limit of 1.5MPa. This is an increase in the vessel capacity by 7%. The results are summarised in Table 1

Thermal Transient Creep

For the thermal transient investigated, the impact of TTC on strain levels is shown to be small. Comparison of the inner wall strain distributions highlight there is very little change when TTC is simulated [10]. A nominal reduction is observed in the E11 (i.e. radial at this location) tensile strain at the top of the buttress on the 270° azimuth [10]. The level of TTC activity in concrete is temperature dependant. Creep initiation occurs at levels above 85°C and activity increases with respect to temperatures in excess of this. However, for the fault transient investigated low temperature distributions dominate, particularly through the thickness of the containment concrete boundary. Hence significant strain re-distribution is not witnessed.

The inclusion of TTC has an effect on vessel displacements. The effects are most pronounced for the radial displacements. TTC is simulated using an effective Young's modulus approach to reduce the material stiffness of the concrete. Thus the restraining effects of the pre-tensioning tendons become more dominant as the concrete stiffness reduces. The increasing dominance of the compressive pre-loading results in the reduced displacements calculated for the TTC analysis.

This investigation considers a fault transient based on a loss of cooling accident for a typical PWR containment. However, for British Advanced Gas-cooled Reactors (AGR), the pre-stressed concrete pressure vessels (PCPV) are expected to experience more elevated and sustained thermal transients. Thus TTC can be expected to be of more significance to the AGRs.

CONCLUSIONS

When the effects of accident temperatures on concrete containments are considered, the following conclusions can be made.

- The elevated temperatures induce significant thermal expansion of the steel liner. The thermal straining of the liner results in rupture at approximately 1.25MPa. This is 14% higher than the rupture pressure of 1.1MPa obtained from the mechanical loading of the limit state test.
- The pre-loaded tendons are well insulated from the peak temperatures experienced in the accident transient. However, the global response of the PCCV increases the pressure required to induce tendon failure from 1.4MPa to approximately 1.50MPa. This is an increase of approximately 7% compared to the limit state test.
- For the accident condition investigated, liner rupture is the initial failure mode. The design intent of liner rupture before catastrophic failure of the containment is maintained.
- If the margin between tendon failure and liner rupture is defined as the ratio of vessel pressurisation required to cause the failures, the margin decreases from 1.27 for pressure only to 1.2 for pressure plus temperature loads.
- The temperature dependent effect of TTC in concrete is simulated using an effective modulus approach. For the accident condition investigated TTC is shown to have a small effect on PCCV strain distributions, but reduced vessel displacements are witnessed.

REFERENCES

[1] Overpressurisation Test of a 1:4 Scale Prestress Concrete Containment Vessel Model, Sandia National Lab., NUREG/CR-6810, SAND2003-0840P, Project Report No. R-SN-P-010, March 2003.
[2] HSE/NNC Pretest Analysis Report for ¼ Scale PCCV Model, NNC Report C5769/TR/002.
[3] Pretest Round Robin Analysis of a Prestressed Concrete Containment Vessel, Sandia National Lab., NUREG/CR-6678, SANDE 00-1535, August 2000.
[4] HSE/NNC PCCV Round Robin Post Test Analysis, NNC Report C6635/TR/001, Issue 01, Dec 2002.
[5] Summary Records of the 2nd meeting of the ISP48 Exercise on Containment Capacity. Madrid, Spain, 19 March 2004. OECD Nuclear Energy Agency IAGE-CONC/ISP48/(04)1. 2 April 2004.
[6] ABAQUS/Standard Version 6.4, ABAQUS/CAE, ABAQUS/Viewer, ABAQUS Inc., USA.
[7] Obayashi Corporation package of construction drawings of PCCV model.
[8] International Standard Problem on Containment Capacity (ISP-48) Phases 1 & 2 NNC Report C11248/TR/001 Issue 2 April 2004.
[9] Structural Performance of PCPV's at Elevated Temperatures. Nuclear Electric plc, EWI-17275/R/008, December 1996.
[10] International Standard Problem on Containment Capacity (ISP-48) Phases 1 & 2 NNC Report C11248/TR/002 Issue 01 December 2004.
[11] An Engineering Data Book – J R Calvert & R A Farrar, 1999.

ACKNOWLEDGEMENTS

The Authors are grateful for the support and encouragement which they have received from Mr Graham Doughty (British Energy) and Dave Shepherd (NII, HSE).

Table 1 Summary of Results: Calculated Pressures (MPa) and Strains (%)

Loading	Cracking		Liner Yield	Liner Rupture	Hoop Tendon Stress		Pressure @ Failure	Free Field Hoop Strain**	Max Radial Displacement***	Mode
	Hoop	Meridional			Yield+	Rupture				
Pressure	0.6	0.6	0.75	1.1*	1.16	1.4!	1.4	0.12%	38.8mm	Liner tearing causing high leakage rates.
Pressure + Temperature	0.6	0.6	0.83	1.25	0.96	1.5	1.25 1.50	0.18%	49.4mm	Liner tearing. Hoop Tendon failure.
Pressure + Temperature with TTC	0.6	0.6	0.82	-	-	-	-	-	-	
LST Test Results	0.59	-	-	0.98	1.02	-	0.98 1.295	0.17% -	28.30mm	Liner Tearing, 1% mass/day leak. Max. Pressure @ 1000% mass/day leak
SFMT Test Results	-	-	-	-	-	1.4	1.4	-	86mm	Structural collapse

* Liner strain of 0.0017 reached at SOL39
! Hoop tendon strain of 0.0034 at the maximum SFMT pressure in tendon H53
** Strains at SOL39 @0.98Mpa
*** Displacement at SOL 14 @1.295Mpa
+ Assumed yield strain of 0.2% obtained from tendon testing at SOL50

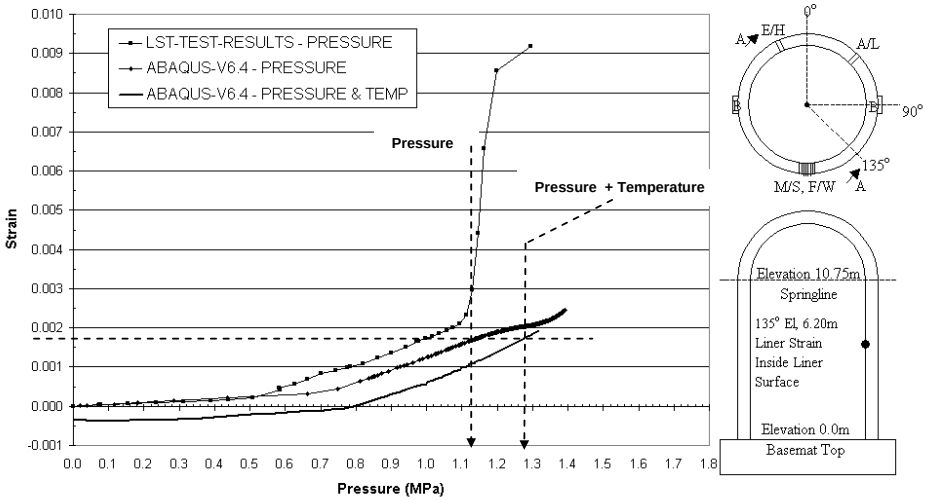

Figure 1 Standard Output Location 39 Hoop Liner Mechanical Strain

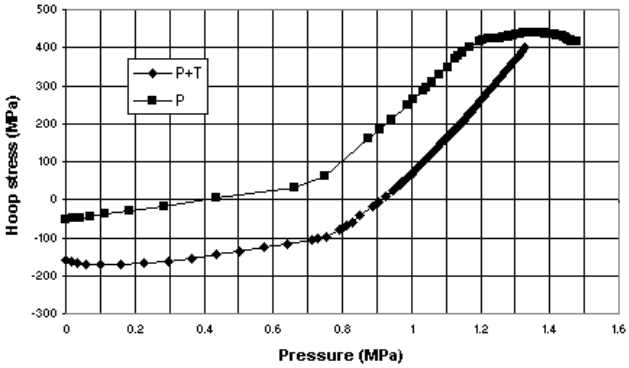

Figure 2 Standard Output Location 39 Hoop Liner Stress

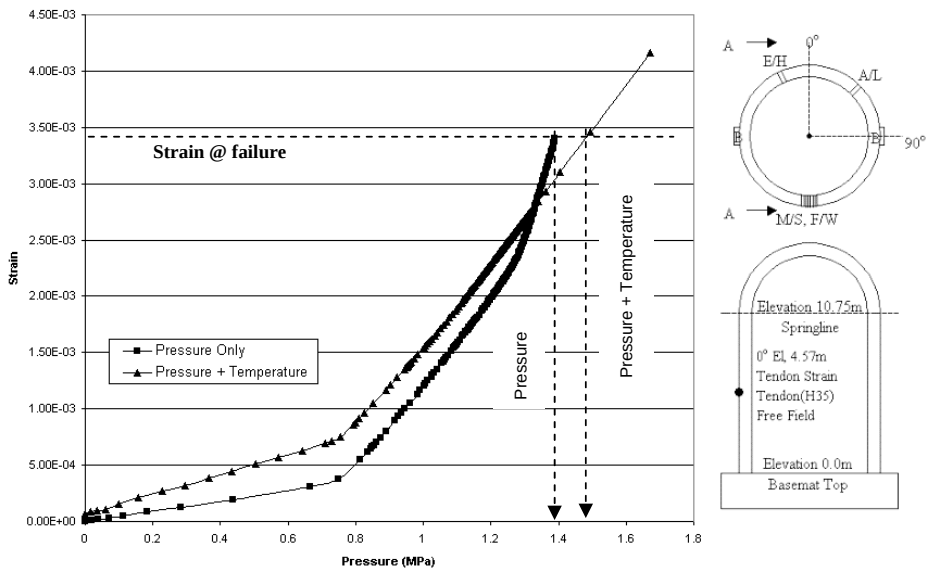

Figure 3 Standard Output Location 53 Hoop Tendon Mechanical Strain

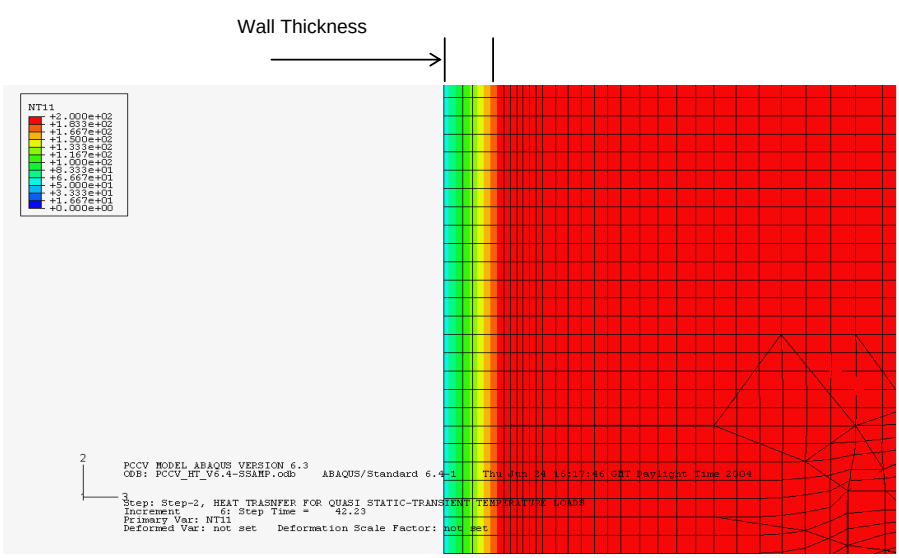

Figure 4 Temperature contour profiles through the cylinder wall thickness